Mechanical Damage Detection With Magnetic Flux Leakage Tools: Modeling the Effect of Localized Residual Stresses

Vijay Babbar, Behrouz Shiari, and Lynann Clapham

***Abstract*—We used three-dimensional (3-D) magnetic finite-element analysis (FEA) to simulate the effect of localized residual stresses on magnetic flux leakage (MFL) signals from a steel plate in the absence of a geometrical defect. We derived the local residual stress patterns from finite-element structural modeling of simulated dents. The magnetic FEA model simulates these localized residual stresses by assigning appropriate directional permeability values to the magnetically anisotropic materials. Considering the necessary simplifications required for magnetic FEA modeling, the simulated MFL patterns are in good agreement with the experimentally observed patterns associated with the stresses around a dent.**

***Index Terms*—Finite-element analysis, magnetic flux leakage, nondestructive evaluation, stress.**

I. Introduction

NONDESTRUCTIVE evaluation of in-service oil and gas pipelines by the magnetic flux leakage (MFL) technique has been the subject of interest for many years [1], [2]. Both experimental methods and computational techniques such as magnetic finite-element analysis (FEA) have been used to study MFL signals from corrosion pits [3]–[7]. Because these defects produce MFL signals mainly due to their geometry, the size and shape of the pit can be obtained by studying the magnitude and shape of the MFL output signal [8]. However, these signals are also affected by the system parameters such as inspection tool type, tool velocity [9], line pressure stress [10]–[13], and magnetic properties of the steel pipe wall.

In addition to corrosion defects, dents or "mechanical damage" in pipelines are also of serious concern. Dents incorporate wall geometry changes as well as localized stress regions. Both the geometry and stress will combine to form an MFL signal—the geometry variations by perturbing the flux path and the residual stresses by changing the local magnetic anisotropy around the dent.

Manuscript received January 24, 2003; revised August 28, 2003. This work was supported by the Gas Technology Institute, U.S., and the Natural Sciences and Engineering Research Council of Canada.

V. Babbar is with Applied Magnetics Group, Physics Department, Queen's University, Kingston, ON K7L 3N6, Canada, on leave from Guru Nanak Dev University, Amritsar, India (e-mail: babbar@physics.queensu.ca).

B. Shiari is with Department of Mechanical and Aerospace Engineering, Carleton University, Ottawa, ON K1S 5B6, Canada, on leave from Guilan University, Rasht, Iran (e-mail: bshiari@mae.carleton.ca).

L. Clapham is with Applied Magnetics Group, Physics Department, Queen's University, Kingston, ON K7L 3N6, Canada (e-mail: lynann@physics.queensu.ca).

Digital Object Identifier 10.1109/TMAG.2003.821121

In order to be able to identify and characterize dents using MFL tools, first we must understand the separate contributions of dent stress and dent geometry to MFL signals. Modeling of *geometry-induced* MFL signals is relatively straightforward, and commercially available finite-element software is available to do this (e.g., ANSYS, Infolytica MagNet). However, finite-element modeling of *stress-induced* MFL signals is far more difficult. This is because stress causes variations in the basic magnetic property of a material—the magnetic permeability. Permeability is a nonlinear function of the applied field. Most magnetic FEA models can account for this nonlinearity, however, stress creates *local permeability variations* in materials, and *also anisotropic permeability*. In order to model stress effects, therefore, a magnetic FEA model must be able to accommodate *locally assigned, anisotropic permeability* functions within a material. The authors have worked closely with Infolytica FEA software manufacturers to accommodate these complex requirements. Although the models are still somewhat crude, this work has produced a number of successful applications of magnetic FEA modeling that examine the effects of stress on MFL signals [7].

In the present study, the magnetic FEA is used to model local dent-induced stress effects on MFL signals. The results are compared with experimentally obtained MFL results from a controlled denting study. The geometry effects are effectively subtracted off in both cases. These geometry effects will be considered in a subsequent paper.

II. The Models

A. Structural FEA Model

A nonlinear structural FEA model using ANSYS software was used for simulating three-dimensional (3-D) residual stress profiles in a dented plate. Fig. 1 shows the model geometry. A round-bottomed punch was used to make a dent of diameter 12 mm and depth 3 mm in a mild steel plate of dimensions 40 mm × 40 mm × 3 mm. Below the plate was a die containing a hole of diameter 18 mm. Only one-quarter of the model was necessary due to symmetry considerations. The interfaces between the die and the plate, and between the plate and the punch were modeled using an automatic surface-to-surface contact algorithm, which uses the material properties of both contacting surfaces to calculate the stiffness of the contact elements. An elastic Coulomb friction law is assumed and

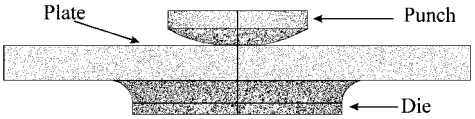

Fig. 1. Geometry of the FEA structural model.

a friction coefficient of 0.15 is assigned to the contacting surfaces. The structural element used to mesh the plate is defined by ten nodes, each having three degrees of freedom at each node (translations in the nodal x, y, and z directions). The elements also have plasticity, creep, swelling, stress stiffening, large deflection, and large strain capabilities. The model is composed of 802 contact elements and 3851 solid structural elements. The stress-strain behavior of the material is described by a bilinear total stress/total strain curve starting at the origin and with positive stress and strain values. A piecewise linear elastic–prefect plastic material model is assumed for the plate with the following parameters: Young's modulus $= 207$ GPa, yield strength $= 160$ MPa, tangent modulus $= 0.112$ GPa, Poisson's ratio $= 0.290$, and density $= 7900\ \text{kg} \cdot \text{m}^{-3}$.

The finite-element stress simulation involved two steps. The first step analyzed the plate behavior during the forming process. The second step involved unloading and determined the amount of residual stress and shape distortion after springback. The static-implicit method, which is based on a Lagrangian description of motion and an elastic-plastic constitutive law, was used for solving the problem, and the Newton–Raphson method was used for solving the equations.

1) Structural FEA Model Results: As an example of the results generated by the modeling, Fig. 2(a)–(c) shows the normal residual stresses in the x and y directions and the shear stresses, respectively. Significant stresses are present in the dent rim region as well as at the dent base. Only the dent rim stresses, which mainly occur within a ring of radius between $r = 12$ and 18 mm, were considered in the present magnetic FEA. Fig. 3 is a schematic illustration of the FEA results in the dent rim, showing that the dent rim stresses are radial; tensile at the top and compressive at the bottom surface. The stresses in the z direction are not considered, since the model indicated that they were an order of magnitude less than those in the x and y directions.

B. Magnetic Finite-Element Analysis Model

Since the aim was to study only stress and not geometry effects, the model consisted of a flat steel plate $(66\ \text{mm} \times 54\ \text{mm} \times 1.6\ \text{mm})$. There was no defect in the plate; however, the magnetic anisotropy was varied in the "dent rim," i.e., the region $r = 12$–18 mm from the "dent center," according to the results obtained in the structural FEA model. Infolytica MagNet6 software was used for drawing as well as solving the model. A Nd–Fe–B magnet with coercivity of $1.6 \times 10^6\ \text{A} \cdot \text{m}^{-1}$ was used to magnetize the steel plate in the x direction. This magnetization level produced a flux density of about 1.8 T in the plate; this corresponds to a high magnetization level during an actual MFL inspection. The fourfold symmetry of the problem facilitated the use of a quarter model, which is shown schematically in Fig. 4 (3-D view) and also in Fig. 5 (side and plan views).

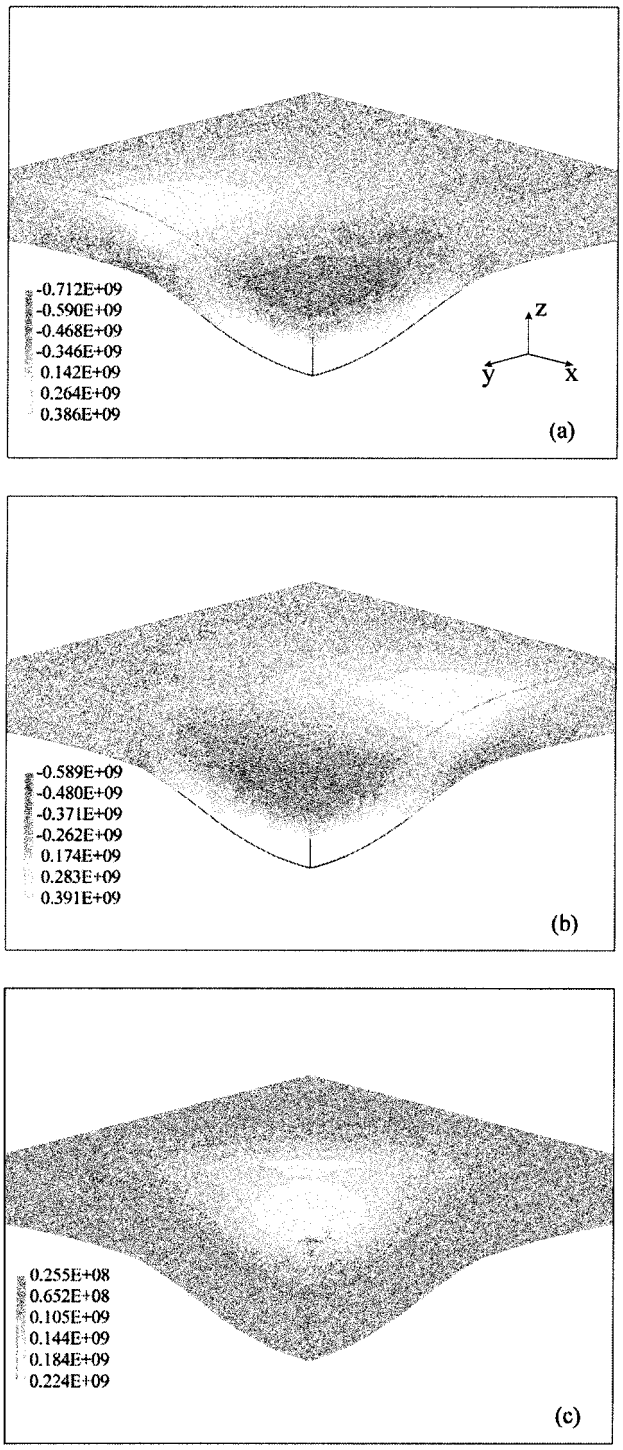

Fig. 2. Residual stresses in a 20 mm × 20 mm × 3 mm quarter section of the structural model. (a) Normal stresses in the x direction. (b) Normal stresses in the y direction. (c) Shear stresses.

The "MFL signal" corresponded to the radial component of the magnetic field at a distance of 0.5 mm above the plate.

In a real material, stress is, of course, a continuous function of position as indicated in Fig. 2; thus, permeability will also vary continuously. However, continuous permeability variations with position are not possible given the current state of FEA development. Thus, in the present model, local permeability variations are accommodated discretely in "blocks" of material, each of

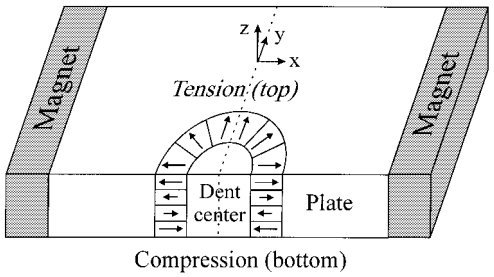

Fig. 3. Schematic illustration of the nature of stresses modeled in one half of the plate. Tensile stresses are developed in the upper half section and compressive stresses in the lower half section of the plate.

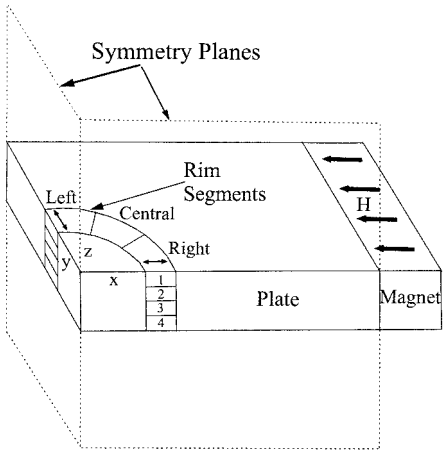

Fig. 4. Schematic 3-D view of the quarter magnetic FEA model.

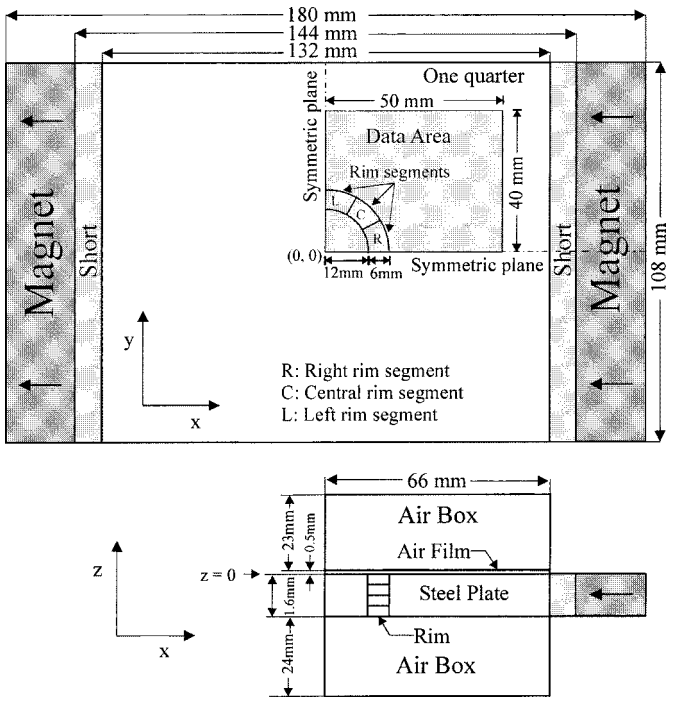

Fig. 5. Schematic plan view (upper) and side view (lower) of the magnetic FEA model (not drawn to scale).

which is assigned a specific anisotropy function. As shown in Figs. 4 and 5, the rim is divided into 12 regions: blocks 1–4 in each of the left, central, and right sections. Each of these regions can be assigned different magnetic permeability functions along each of the orthogonal x, y, and z directions in order to account for the local residual stress. The way in which stress effects are accounted for in the magnetic FEA model is discussed below.

1) Accounting for Stress Using Magnetic Anisotropy Variations: Since steel, in general, has a positive magnetostriction coefficient, 180° domains will tend to align their magnetic easy axis closest to, and ultimately rotate it toward, the direction of the applied tensile stress. This increases the magnetic permeability in the tensile stress direction. Conversely, an applied compression will increase the magnetic permeability in a direction transverse to the stress axis.

The Infolytica MagNet6 software allows for 3-D nonlinear anisotropic FEA calculations with customer-supplied magnetization functions. Since high axial fields are used, it is assumed that magnetization must always be in the field direction, and that it can be described as an arc tangent of the field, with the B–H curve approximated as

$$B = \mu_0 \left[\frac{2M_s}{\pi} \tan^{-1} \left(\frac{H}{H_k} \right) + H \right] \tag{1}$$

where μ_0 is the permeability of free space, H_k is a directionally dependent anisotropy parameter, M_s is the saturation magnetization equal to 1700 kA $\cdot$ m^{-1} (for this steel), and H is assigned to be 27 500 A $\cdot$ m^{-1}. This equation is used to calculate the components of B by assigning values of H_k in each of the three orthogonal different directions.

Using (1), the maximum permeability μ_m can be shown to be

$$\mu_m = \mu_0 \left(\frac{2M_s}{\pi H_k} + 1 \right). \tag{2}$$

Thus, smaller values of H_k imply higher permeability.

Since tensile stress increases and compressive stress decreases the permeability in the stress direction, we vary the H_k in a specific (x, y, or z) direction to simulate applied stress. For example, one can simulate a tensile stress in the y direction by decreasing H_k in that direction and/or by increasing H_k along the other two orthogonal directions. In general, the anisotropy parameter in any given direction is expressed as

$$H_k = H_{kx}\alpha_x^2 + H_{ky}\alpha_y^2 + H_{kz}\alpha_z^2 \tag{3}$$

where H_{kx}, H_{ky}, and H_{kz} are the three orthogonal anisotropy parameters, and α_x, α_y, and α_z are the cosines of the field vector in that direction.

In the present study, for the isotropic (no stress) case, a value of $H_{k(xyz)} = 9000$ A $\cdot$ m^{-1} was assigned to all three directions in all parts of the model (the main plate, the 12 dent rim regions, and the dent center). The solution of the model indicated that this H_k value corresponds to a relative permeability of 50.4 and a flux density of 1.74 T inside the plate for an applied axial field of about 27 500 A $\cdot$ m^{-1}. Outside the plate at $z = 0.5$ mm, the radial flux density was calculated to be $\mu_0 H = 0.038$ T.

As mentioned above, tensile and compressive stresses were incorporated by assigning $H_{k(xyz)}$ values that were lower or higher, respectively, than 9000 A $\cdot$ m^{-1}. Table I shows the values of B and $\mu_r (= \mu/\mu_0)$ obtained by using (1) for the range of $H_{k(xyz)}$ values used in the present study.

TABLE I
FLUX DENSITY INSIDE THE STEEL PLATE AND RELATIVE PERMEABILITY OF THE PLATE VERSUS H_k AS GIVEN BY (1) WITH $H = 27\,500$ A $\cdot$ m^{-1} AND $M_s = 1.7 \times 10^6$ A $\cdot$ m^{-1}

H_k (A.m^{-1})	B (T)	μ_r (= μ/μ_0)
2,000	2.07	60.0
5,500	1.90	55.0
9,000	1.74	50.4
12,500	1.59	46.0
16,000	1.45	42.1

The values of H_{kx}, H_{ky}, and H_{kz} for any region of the magnetic model are decided on the basis of the FEA residual strain results presented in Section II-A. The MFL results for various stress combinations are considered below.

2) MFL Results Due to High Tensile Stresses in Top Left and Right Dent Rim Segments: FEA structural modeling identified high tensile x-direction strain in the top right, and high tensile y-direction strain in the top left segments of the dent rim (Figs. 2 and 3). The top two blocks of the right rim segment were assigned anisotropy parameters H_{kx}, H_{ky}, and H_{kz} of 2000, 9000, and 9000 A $\cdot$ m^{-1}, respectively, thus increasing the permeability in the x direction. Similarly, the top two blocks of the left ring segment were assigned H_{kx}, H_{ky}, and H_{kz} values of 9000, 2000, and 9000 A$\cdot$m^{-1}, giving it an increased y-direction permeability.

Fig. 6 shows the axial profile, contour map, and surface plot of B_z at z equal to 0.5 mm for the conditions described above. These results are "background-subtracted," i.e., the corresponding isotropic results have been subtracted off in order to examine only the strain contribution to the signal. As seen in Fig. 6, the tensile stress in these regions creates a significant radial MFL peak between the left and central sections. Interestingly, the same result is obtained even when the top right regions are assigned isotropic values, indicating that an increased permeability must facilitate a direction change of the field in the plate in order to alter the MFL signal.

3) MFL Results Due to High Compressive Stresses in Bottom Left and Right Dent Rim Segments: The FEA structural modeling revealed high compressive x-direction strain in the bottom right, and also high compressive y-direction strain in the bottom left segments of the dent rim (Figs. 2 and 3). As with the tensile strain regions discussed in the previous section, stress effects from these compressive regions were independently modeled using MagNet to examine their influence on the MFL signals. The compressive strain was modeled by assigning $H_{ky} = 16\,000$ A $\cdot$ m^{-1} to the bottom two blocks of the left region, and $H_{kx} = 16\,000$ A $\cdot$ m^{-1} to the bottom two blocks of the right region. The results, subtracted from the isotropic case, are shown in Fig. 7 and indicate a small but broad minimum that is centered at nearly the same location as the maximum for the case of tensile stresses. While the opposite polarity results from compressive rather than tensile stresses, the low value reflects the larger distance traversed by the leakage signals through the plate before their detection.

4) MFL Results Due to Combined Tensile and Compressive Stresses in the Left and Right Dent Rim Segments: In this model, the anisotropies described in Sections II-B2 and II-B3 are combined, with tensile stress anisotropies at the top and compressive stress anisotropies at the bottom of the left and right dent rim regions. The values of H_{kx} and H_{ky} are the same as those used before. The results are shown in Fig. 8. As expected, the tensile effects at the top (modeled independently in Fig. 6) dominate the pattern, creating a large MFL peak at the central/left boundary position. The main effect of the compressive regions is to slightly reduce the peak amplitude.

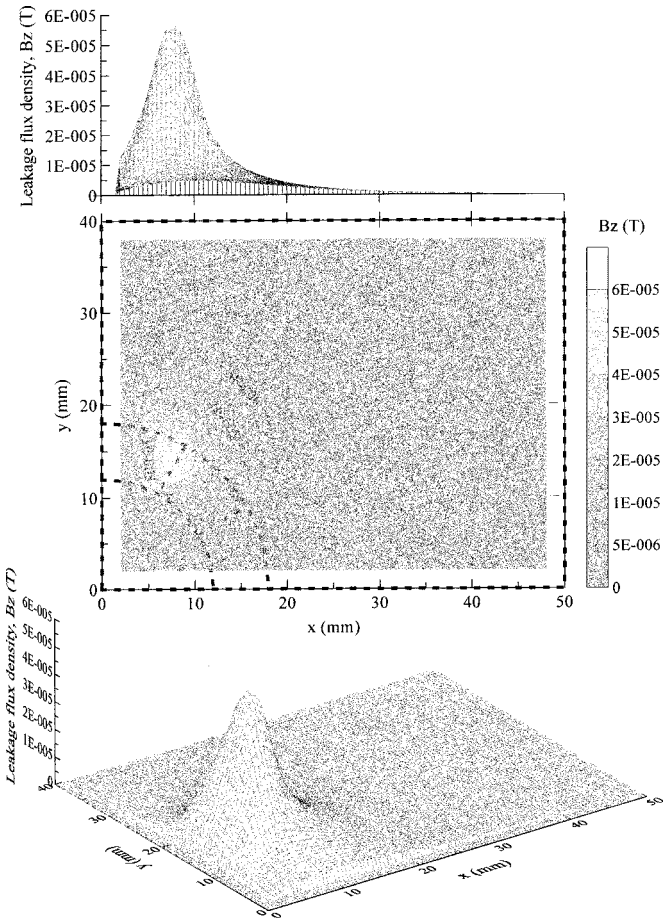

Fig. 6. Axial profile (upper), contour map (middle), and surface plot (lower) at 0.5 mm above the top surface of the sample. Tensile stresses were simulated in the top two blocks of the left as well as right rim segments.

5) MFL Results Due to Shear Stresses in the Central Dent Rim Segments: Fig. 2(c) indicates that shear stresses are present in the central region of the dent rim. Unfortunately, simulation of shear stress effects was not possible, since H_k values could only be assigned to either x, y, or z direction. However, the effect of stress anisotropy in the central rim region was examined by studying two "extreme" cases, first by assigning it x anisotropy and second by assigning it y anisotropy. In both cases, the left and right rim regions were assigned the anisotropies as discussed in Section II-B4.

The first case of x anisotropy in the central dent rim segments yields the same results as shown in Fig. 8, when the central region was isotropic. Assigning a y anisotropy has a more significant effect—causing the peak in Fig. 8 to rotate by about 25° clockwise, to a position roughly in the middle of the central region. The magnitude of the peak changed little.

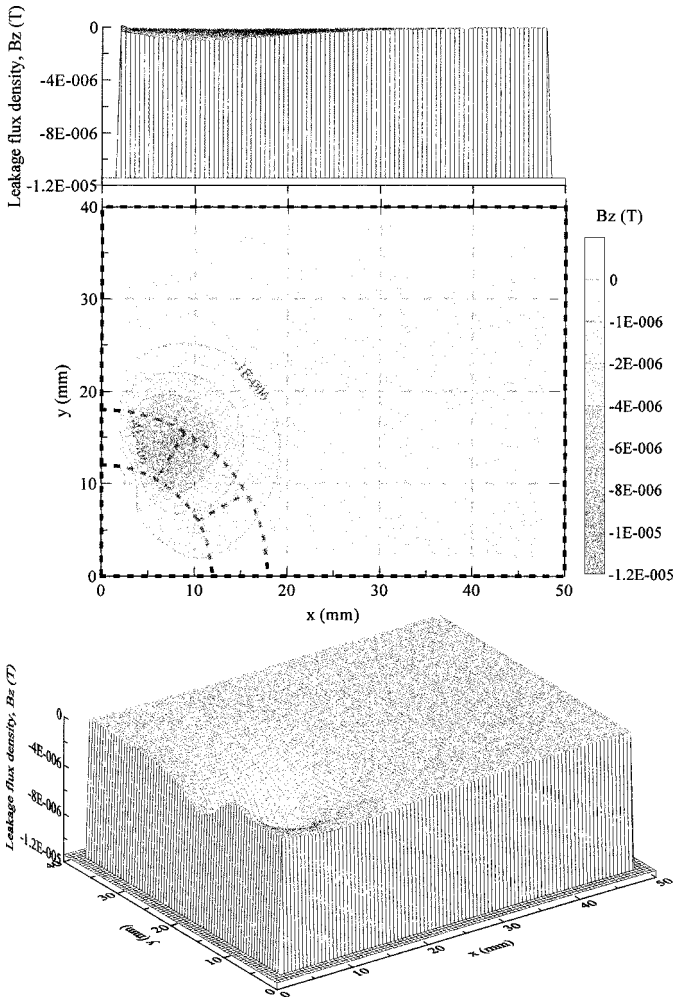

Fig. 7. Axial profile (upper), contour map (middle), and surface plot (lower) at 0.5 mm above the top surface of the sample. Compressive stresses were simulated in the bottom two blocks of the left as well as right rim segments.

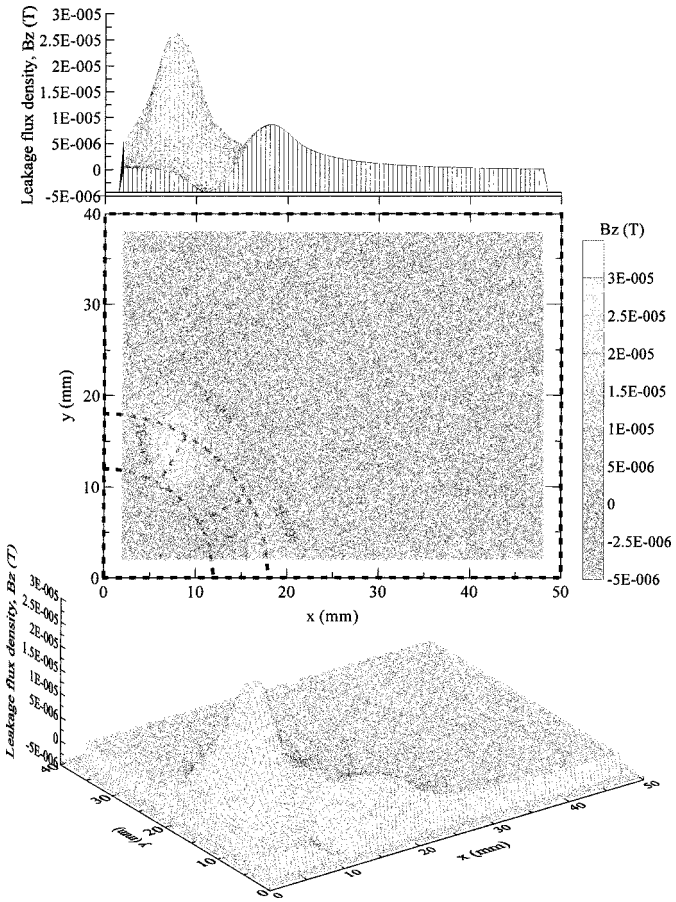

Fig. 8. Axial profile (upper), contour map (middle), and surface plot (lower) at 0.5 mm above the top surface of the sample. Tensile stresses were simulated in the upper half and compressive stresses in the lower half of the left as well as right rim segments.

Therefore, although it could not be directly modeled, assigning a shear stress anisotropy (rather than an x or y anisotropy) to the central region was expected to produce a slight (approximately 10°–15°) clockwise shift in the peak position shown in Fig. 8.

III. Experimental Details and Results

Experimental MFL testing was carried out for comparison with the FEA modeling results. Samples of mild steel of approximate dimensions 200 mm × 150 mm × 1.6 mm were first sanded and then heated at 500 °C for 1 h to remove any residual stresses that might be present before denting. An experimental tool and die of similar dimensions to the FEA stress model (see Section II-A and Fig. 1) was used to produce dents, which were made by using a hydraulic press at a ram speed of 6 mm/s in constant displacement mode with an applied force of about 16–17 kN.

MFL measurements were made after denting at the top surface of the plate. The MFL experimental arrangement was similar to that described in a previous work [15] except that the sample in the present work was a flat plate instead of a pipe. Magnetic flux was introduced into the plate by a Nd–Fe–B permanent-magnet circuit. The MFL signal was detected by using a Hall probe, which was scanned over a 40 mm × 40 mm area around the dent on top of the dented surface. Finally, a 3-D plotting package (Surfer 7.0) from Golden Software was used for obtaining surface and contour maps.

The contribution of the stress to the experimental MFL dent signal was obtained in the following manner: MFL measurements were made after the dent was created. It was followed by the heating of the dented plate at 500 °C for 1 h. Earlier work showed that this removes residual stresses and all magnetic effects associated with them [16]. The MFL measurements were then repeated for the dent. Finally the "after-heating" MFL scan data was subtracted from the "before-heating" scan data. This produced the MFL pattern associated with the dent stresses only, as shown in Fig. 9(a).

The magnetic FEA (stress-only) result is shown Fig. 9(b). This same data was shown in Fig. 8, but is reproduced here for direct comparison with the experimental data. A comparison of the experimental [Fig. 9(a)] and FEA-modeled [Fig. 9(b)] results indicates that they are qualitatively similar—both display positive MFL peaks in the upper rim region. The experimental MFL peak appears to lie slightly clockwise compared to the FEA peak, which is expected since the FEA result does not include the shear stress anisotropy associated with the central

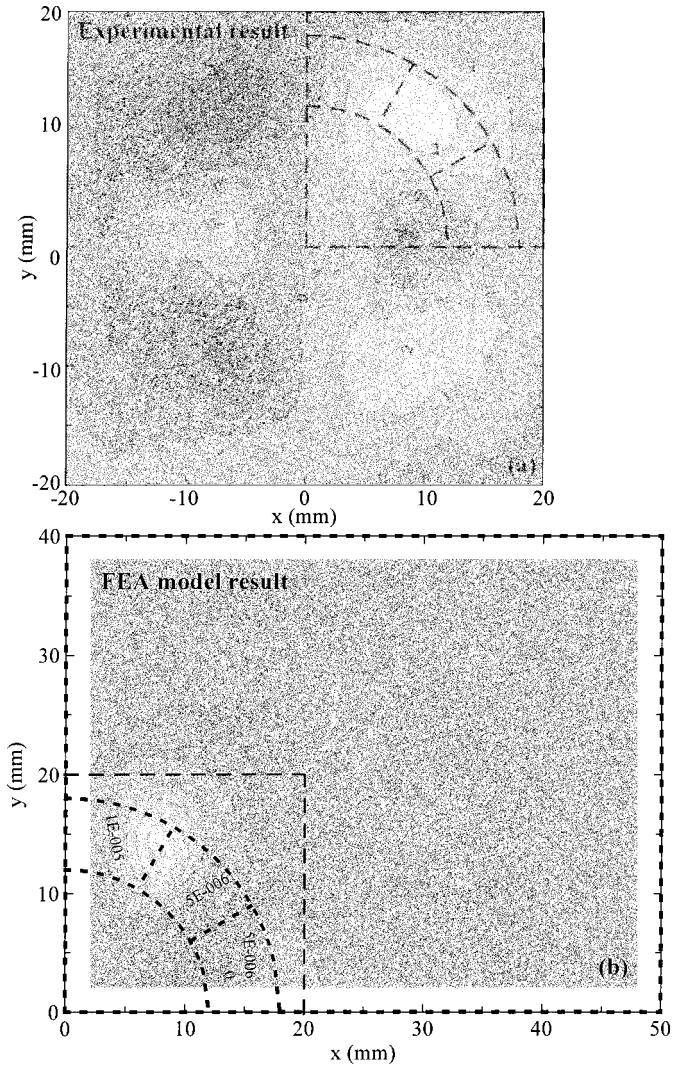

Fig. 9. Contour plots of B_z generated by dent rim residual stresses, for (a) the experimental MFL result and (b) the magnetic FEA MFL result. Comparison should be made in the regions surrounded by dotted lines. The dotted arc indicates the region of dent rim stresses in both cases. The units for the numbers are 10^{-4} T in (a) and T in (b). The signal magnitudes in (a) and (b) are not directly comparable due to use of oversimplified stress zones and limitations in defining material properties of the sample and the magnet in the FEA model.

dent region (Section II-B5). If the shear stress effects could be included, then we expect that the FEA and experimental peak locations would closely coincide.

IV. Summary and Conclusion

Modeling of stress effect on MFL signals is extremely difficult, and to our knowledge, it is the first attempt to model MFL signals arising from dent stresses. Results indicate that the tensile stresses in the dent rim, being closer to the measurement surface, make a more significant contribution to the signal than the compressive stresses at the opposite side of the plate. The effects are expected to be reversed if MFL measurements are made at the lower side of the plate.

The experimental stress-generated MFL results were in good qualitative agreement with the FEA-modeled results. We do not expect full quantitative agreement because of crude approximations used in drawing stress zones necessitated by model limitations, and simplifying assumptions made regarding the material properties of the sample and the magnet in the FEA model. Shear stresses could not be incorporated into the model at this stage, but estimation of their effects appeared to prove consistent with the experimental data. Finally, it is interesting to note that the good agreement between experimental and FEA modeling was obtained without considering the stresses in the base of the dent as well as along the z direction in the FEA model. This suggests that, when measuring the experimental MFL signal at the top surface of the plate, the dent base stresses have little effect. They are expected to contribute considerably more to an MFL measurement made at the bottom surface of the plate, and modeling work is under way to examine their effects.

References

[1] D. L. Atherton, "Magnetic inspection is key to ensuring safe pipelines," *Oil Gas J.*, vol. 87, no. 32, pp. 52–61, 1989.

[2] L. Clapham and D. L. Atherton, "Magnetic flux leakage inspection of oil and gas pipelines," in *Proc. Int. Symp. Materials for Resource Recovery and Transport*, Calgary, AB, Canada, Aug. 1998, pp. 313–326.

[3] N. Ida and W. Lord, "3-D finite element predictions of magnetostatic leakage fields," *IEEE Trans. Magn.*, vol. MAG-19, pp. 2260–2265, Sept. 1983.

[4] D. L. Atherton, "Finite element calculations and computer measurements of magnetic flux leakage patterns from pits," *Br. J. Non-Destr. Test.*, vol. 30, no. 3, pp. 159–162, 1988.

[5] P. A. Ivanov, Z. Zhang, C. H. Yeoh, L. Udpa, Y. Sun, S. S. Udpa, and W. Lord, "Magnetic flux leakage modeling for mechanical damage in transmission pipelines," *IEEE Trans. Magn.*, vol. 34, pp. 3020–3023, Sept. 1998.

[6] L. Clapham, K. Mandal, R. Sabet-Sharghi, D. L. Atherton, T. Holden, A. Teitsma, P. Laursen, and B. Mergeles, "Variations in stress concentration factors near simulated corrosion pits as monitored by magnetic flux leakage, magnetic Barkhausen noise and neutron diffraction," in *Proc. Int. Pipeline Conf.*, Calgary, AB, Canada, June 1998, pp. 505–512.

[7] W. Mao, C. Mandache, L. Clapham, and D. L. Atherton, "The effect of bulk stresses on magnetic flux leakage signals," *Insight*, vol. 43, no. 10, pp. 688–691, 2001.

[8] T. W. Krause, R. M. Donaldson, R. Barnes, and D. L. Atherton, "Variations of stress-dependent magnetic flux leakage signal with defect depth and flux density," *Non-Destr. Test. Eval. Int.*, vol. 29, no. 2, pp. 79–86, 1996.

[9] D. L. Atherton, C. Jagdish, P. Laursen, V. Storm, F. Ham, and B. Scharfenberger, "Pipeline inspection—tool speed alters MFL signals," *Oil Gas J.*, vol. 88, pp. 84–86, 1990.

[10] P. Laursen and D. L. Atherton, "Effects of line pressure stress on magnetic flux leakage patterns," *Br. J. Non-Destr. Test.*, vol. 34, no. 6, pp. 285–288, 1992.

[11] R. Barnes and D. L. Atherton, "Effects of bending stresses on magnetic flux leakage patterns," *Non-Destr. Test. Eval. Int.*, vol. 26, no. 1, pp. 3–6, 1993.

[12] C. Hauge and D. L. Atherton, "Line pressure stress affects MFL signals," *Oil Gas J.*, vol. 94, no. 12, pp. 92–96, 1996.

[13] C. R. Coughlin, L. Clapham, and D. L. Atherton, "Effects of stress on MFL responses from elongated corrosion pits in pipeline steel," *Non-Destr. Test. Eval. Int.*, vol. 33, pp. 181–188, 2000.

[14] C.-G. Stefanita, D. L. Atherton, and L. Clapham, "Plastic versus elastic deformation effects on magnetic Barkhausen noise in steel," *Acta Mater.*, vol. 48, pp. 3545–3551, 2000.

[15] V. Babbar and L. Clapham, "Residual MFL—a possible tool for studying pipeline defects," *J. Nondest. Eval.*, submitted for publication.

[16] L. Clapham, V. Babbar, T. Rahim, and D. Atherton, "Detection of mechanical damage using the magnetic flux leakage technique," in *Proc. 4th Int. Pipeline Conf.*, Calgary, AB, Canada, Sept. 2002, IPC2002-27 142.

Vijay Babbar received the M.Sc. degree in physics from Guru Nanak Dev University, Amritsar, India, in 1983 and the Ph.D. degree from Indian Institute of Technology, New Delhi, India, in 1990, where he worked on hot pressed ferrites for magnetic recording.

He worked for one year as Scientist "B" at the Defence Laboratory, Jodhpur, India, and for two years as Lecturer at Thapar Institute of Engineering and Technology, Patiala, India. He joined the faculty of the Applied Physics Department, Guru Nanak Dev University in 1992, where he worked on development and characterization of ferrite-epoxy microwave absorbers. Since 2001, he has been a Postdoctoral Fellow in the Applied Magnetics Group, Queen's University, Kingston, ON, Canada. His current research interests include experimental magnetic flux leakage studies and the finite-element modeling of defects in oil and gas pipelines.

Dr. Babbar is a Life Member of the Materials Research Society of India.

Behrouz Shiari received the B.S., M.S., and Ph.D. degrees in mechanical engineering from Amirkabir University of Technology (Tehran Polytechnic), Tehran, Iran, in 1986, 1988, and 1999, respectively.

He was a Member of Faculty at Guilan University, Rahst, Iran, for seven years before obtaining the Ph.D. degree, and has held the position of Assistant Professor since 1999. From 2000 to 2002, he was a Postdoctoral Fellow at Queen's University, Kingston, ON, Canada, where he designed, modeled, and tested a miniature force sensor for mechanical pulp refiners that was filed as a patent. He is currently a Researcher working on multiscale modeling of plasticity and fracture in materials at Carleton University, Ottawa, ON, Canada. His teaching and research interests are nonlinear finite elements, coupled numerical simulation of nanostructures, and piezoelectrics.

Lynann Clapham received the undergraduate degree from Wollongong University, Wollongong, Australia, in 1982 and the Ph.D. degree from Queen's University, Kingston, ON, Canada, in 1989, both in metallurgical engineering.

While pursuing the undergraduate degree, she concurrently worked at Australian Iron and Steel (AIS) in the Basic Oxygen Steelmaking area. After graduation, she worked for another couple of years as a technical officer in Plate Products Development at AIS before coming to Queen's University. After obtaining the Ph.D. degree, she accepted a Research Associate position in the Queen's University Physics Department, working both in the Applied Mathematics Group (AMG) and in the Accelerator-based Materials Science. She joined the faculty of the Physics Department, Queen's University, in 1997. She now runs the AMG, specializing in research and development in pipeline nondestructive evaluation (NDE). Her specific area of expertise is the NDE of stress and the influence of stress on magnetic flux leakage behavior.